Articles

Structural Basis of the Thrombin Selectivity of a Ligand That Contains the Constrained Arginine Mimic (2*S*)-2-Amino-(3*S*)-3-(1-carbamimidoyl-piperidin-3-yl)-propanoic Acid at P1

Lakshmi S. Narasimhan,*,† J. Ronald Rubin,† Debra R. Holland,† Janet S. Plummer,† Stephen T. Rapundalo,† Jeremy E. Edmunds,† Yves St-Denis,‡ M. Arshad Siddiqui,‡ and Christine Humblet†

Parke-Davis Pharmaceutical Research, Division of Warner-Lambert Company, 2800 Plymouth Road, Ann Arbor, Michigan 48105, and BioChem Therapeutic Inc., 275 Boul. Armand-Frappier, Laval, Quebec, Canada H7V 4A7

Received April 29, 1999

We have studied the thrombin and trypsin complexed structures of a pair of peptidomimetic thrombin inhibitors, containing different P1 fragments. The first has arginine as its P1 fragment, and the second contains the constrained arginine mimic (2*S*)-2-amino-(3*S*)-3-(1-carbamimidoyl-piperidin-3-yl)-propanoic acid (SAPA), a fragment known to enhance thrombin/trypsin selectivity of inhibitors. On the basis of an analysis of the nonbonded interactions present in the structures of the trypsin and thrombin complexes of the two inhibitors, the calculated accessible surfaces of the enzymes and inhibitors in the four complexes, data on known structures of trypsin complexes of inhibitors, and factor Xa inhibitory potency of these compounds, we conclude that the ability of this arginine mimic to increase thrombin selectivity of an inhibitor is mediated by its differential interaction with the residue at position 192 (chymotrypsinogen numbering). Thrombin has a glutamic acid at residue 192, and trypsin has a glutamine. The analysis also suggests that this constrained arginine mimic, when present in an inhibitor, might enhance selectivity against other trypsin-like enzymes that have a glutamine at residue position 192.

Introduction

Blood coagulation is the result of a cascade of enzymatic activation resulting in the production of thrombin (factor IIa) in the penultimate step.[1] Thrombin catalyzes the conversion of fibrinogen to fibrinopeptides, activates factor XIII which in turn cross-links the fibrinopeptides to form the clot, and is also a potent stimulator of platelet aggregation.[2] This multiple role in thrombosis makes thrombin an important target for therapeutic agents designed for thrombus prevention.[3,4] There has been considerable interest in the design and development of potent, safe, and orally bioavailable thrombin inhibitors as anticoagulants for treating a variety of clotting disorders.[5−13]

Thrombin is a serine protease and has remarkable similarity in overall three-dimensional structure to the digestive serine proteases trypsin and chymotrypsin.[14,15] Trypsin and thrombin share a common primary specificity for proteolysis next to arginine or lysine residues. Structural data on thrombin and trypsin have demonstrated the strong resemblance in their substrate sites, and many small organic inhibitors are comparably active against both the enzymes.[16,17] For this reason, no or low inhibition of trypsin is viewed as a required condition for a compound to be a successful orally bioavailable thrombin inhibitor.

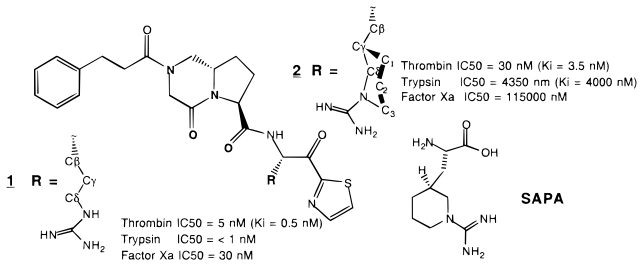

Figure 1. Structures of **1** and **2** and data for their inhibition of the enzymatic activity of thrombin, trypsin, and Factor Xa.

Several cyclic, constrained arginine analogues that target the arginine binding S1 pocket of these enzymes have been explored and are known to bind to these enzymes with high potency.[18] A specific mimic, derived from (2*S*)-2-amino-(3*S*)-3-(1-carbamimidoyl-piperidin-3-yl)-propanoic acid (referred to in this manuscript as SAPA, see Figure 1), was shown to add significant thrombin/trypsin selectivity to inhibitors when compared to their arginine analogues in two different classes of compounds.[19−22]

In this paper we present a study that investigates the structural basis of the thrombin selectivity of SAPA in comparison to arginine. We present details of the X-ray crystal structures of the trypsin and thrombin complexes of two compounds, **1**[23] and **2**[24] (see Figure 1), which contain the P1[25] fragments, argininine and SAPA,

* To whom correspondence should be addressed. Tel: 734-622-2806. Fax: 734-622-2782. E-mail: lakshmi.narasimhan@wl.com.
† Parke-Davis Pharmaceutical Research.
‡ BioChem Therapeutic Inc.

10.1021/jm990216f CCC: $19.00
Published on Web 01/26/2000

respectively. The two compounds differ only in their P1 fragments. In chemical terms, the only difference between **1** and **2** is the presence of a trimethylene bridge, $C_1C_2C_3$ (shown in bold in Figure 1) in **2** and its absence in **1**. A study of the nonbonded interactions present in the structures of the trypsin and thrombin complexes of the two compounds, an analysis of calculated accessible surfaces of the enzymes and inhibitors in the four complexes, additional data on known structures of trypsin complexes of inhibitors, and factor Xa inhibitory potency of these compounds are discussed, and together they provide a convergent description of the factors that contribute to the selectivity of SAPA. Such an understanding could lead to the design of modifications that preserve/enhance the selectivity characteristics of this moiety and could serve to be of general applicability in the design of inhibitors for other serine protease targets.[26]

Results and Discussion

Enzyme Inhibition. Inhibition values of substrate catalysis in vitro by **1** and **2** for the enzymes thrombin, trypsin, and factor Xa are given in Figure 1. Compounds **1** and **2** inhibit thrombin with IC_{50} values of 5 nM (K_i = 0.6 nM) and 30 nM (K_i = 3.5 nM), respectively, suggesting that the introduction of the trimethylene bridge in the P1 fragment of **2** has a small impact on thrombin binding. In contrast, the trypsin inhibitory IC_{50} for **1** and **2** are <1 nM (K_i not measured) and 4350 nM (K_i = 4000 nM), respectively, showing a 4350-fold reduction in trypsin potency. The net effect of the replacement of arginine by SAPA is a 145-fold selective inhibition of thrombin over trypsin. Data on factor Xa inhibition of **1** and **2** are included in Figure 1 to facilitate a later discussion on the relative effects of sequence differences between thrombin and trypsin on the observed selectivity of **2**. The factor Xa activity of **2** drops 3800-fold when compared to that of **1**, which is an inhibition pattern similar to that seen with trypsin.

X-ray Crystallographic Structures of Complexes. To gain a comprehensive understanding of the factors that influence the binding of **1** and **2** to thrombin and trypsin, the thrombin- and trypsin-bound complexes of both the compounds were subjected to X-ray crystallographic studies (for full crystallographic details, see the Experimental Section). The complexes were obtained by soaking the inhibitors into preformed crystals, and the structures were refined to 2.5 Å resolution in the case of thrombin complexes and 1.7 Å resolution for the trypsin complexes. The structures were refined to an *R*-factor of at least 21%, and high occupancy and well-defined difference density were seen for a molecule of the inhibitor in the active site in all the cases.

Structural Details of Thrombin Complexes of 1 and 2. A schematic, summarizing the X-ray crystallographic results for **1** bound to thrombin, is shown in Figure 2. The arginine of **1** binds in the S1 pocket. The thiazole binds in the S1′ prime pocket, and the thiazole nitrogen is positioned to make a hydrogen bond to His57Nϵ of thrombin. The ketocarbon is covalently bonded to Ser195Oγ, and the ketooxygen fits in the oxyanion hole comprised of Ser195NH and Gly193NH. The backbone nitrogen of the arginine fragment of **1** hydrogen bonds to Ser214O. The bicyclic template fits

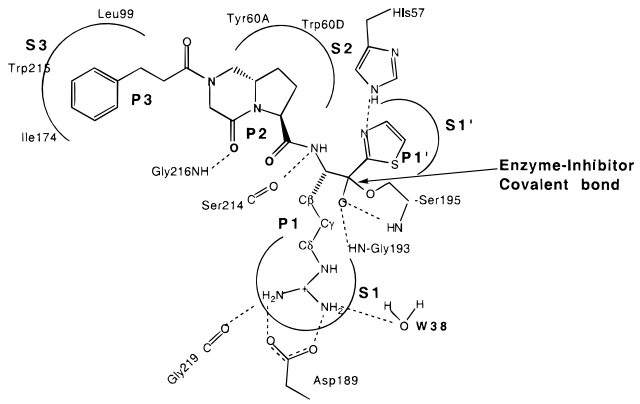

Figure 2. Schematic of the binding of **1** in the thrombin substrate site as seen by X-ray crystallography. A covalent bond is formed between the Ser195 side chain oxygen and the inhibitor (shown). Essential elements of the S3, S2, S1, and S1′ pockets of the enzyme are included. The apportioning of the inhibitor into P3, P2, P1, and P1′ fragments is approximate since the nomenclature is designed to describe peptide substrates and not small molecule inhibitors.

in the S2−S3 pocket in a hydrophobic cavity formed by side chains of Leu99, His57, Tyr60A, and Trp60D. The template carbonyl oxygen hydrogen bonds to Gly216N. The phenylpropanoyl group fits in the distal hydrophobic cavity amidst Ile274, Trp215, and Leu99 side chains positioned orthogonally to the indole ring of Trp215.

The orientation of the P1′ (thiazole), P2 (five-membered ring of the bicyclic template), and P3 (phenylpropanoyl) fragments of the inhibitor in the respective enzyme subsites is remarkably similar in the thrombin and trypsin complexes of **1** and **2** as shown in Figures 5 and 6. This suggests that the binding differences seen for the arginine and SAPA fragments can account for the origin of the selectivity of **2**.

The details of binding in S1 and vicinity, seen in the structural complex of thrombin and **1**, are shown schematically in Figure 3a and stereographically in Figure 5. The amidine end of the arginine fragment is engaged in a salt bridge to Asp189COO^- and is further hydrogen bonded to Gly219O and to a solvent molecule W38. The internal guanidine nitrogen hydrogen bonds to a water molecule (W65) which is hydrogen bonded to Glu192COO^- as well. The P2 C═O of the inhibitor hydrogen bonds to water molecule W64.

The hydrogen bond pairs formed in the S1 pocket of the thrombin−**2** complex are shown in Figure 3b and bear strong similarity to those for the arginine fragment of **1**, in Figure 3a. The boxed segments of Figure 3a,b highlight the notable differences seen for **1** and **2** in their thrombin complexes. First, due to the trimethylene bridge in **2**, the internal nitrogen of the guanidine is now fully substituted and is not able to hydrogen bond to solvent (contrast thrombin−**1** complex). This results in the displacement of water W65 and the elimination of a water-mediated hydrogen bond between protein and inhibitor. Second, the Glu192 side chain has moved to a slightly different position allowing it to make VDW contact with two of the bridge methylene carbons while also hydrogen bonding to both water W57 and Glu192N. The small differences in the position of Glu192 in the two complexes is illustrated by the significant overlap of their Connolly surfaces, as shown in Figure 5. The enzyme does not shift significantly elsewhere when

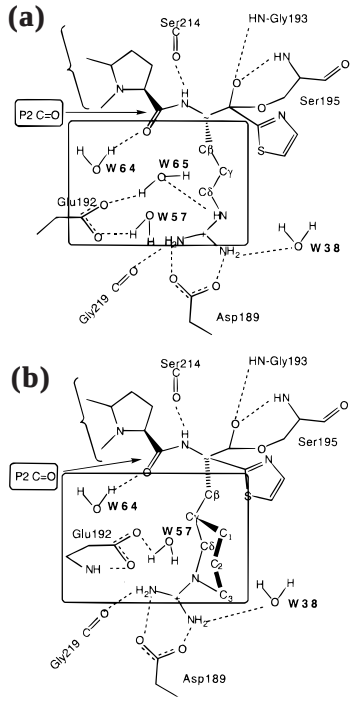

Figure 3. Schematic of the binding seen in and around the S1 pocket in the X-ray structure of the thrombin complexes of **1** (a) and **2** (b). Enzyme inhibitor interactions covering the phenylpropanoyl and bicyclic portion of the inhibitor are excluded. The portion of the hydrogen bonding network containing differences between **1** and **2** are highlighted with a box.

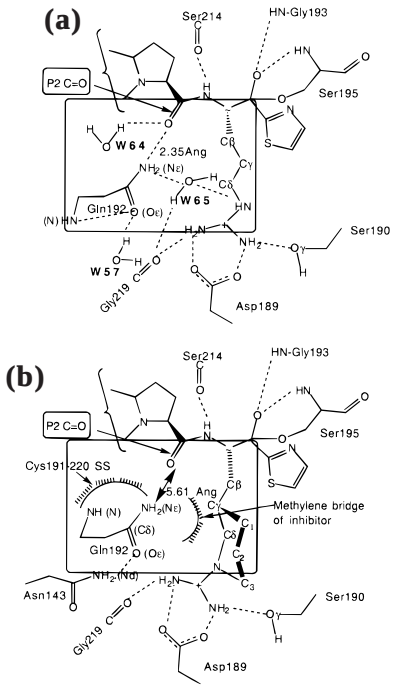

Figure 4. Schematic of the binding seen in and around the S1 pocket in the trypsin complexes of **1** (a) and **2** (b). Enzyme inhibitor interactions covering the phenylpropanoyl and bicyclic portion of the inhibitor are excluded. The portion of the hydrogen bonding network containing differences between **1** and **2** are highlighted with a box.

compared to the thrombin−**1** complex. This remarkable similarity in binding, attenuated by what seem to be minor differences, is consistent with the observed modest change in IC_{50} from 5 nM to 30 nM.

Structural Details of Trypsin Complexes of 1 and 2. The hydrogen bonds in S1 and vicinity in the trypsin complex of **1** and **2** are shown schematically in parts a and b of Figure 4, respectively, and stereographically in Figure 6. The binding seen for the arginine fragment of **1** includes the two hydrogen bond salt bridge to Asp189COO^- and one hydrogen bond each to Gly219O and Ser190Oγ. The internal nitrogen of the guanidine hydrogen bonds to a water molecule (W64 in Figure 4a). This water molecule also hydrogen bonds to Gly219O and Gln192Nϵ, effectively bridging the internal guanidine nitrogen and Gly219O. There is a strong hydrogen bond between Gln192Nϵ and the P2 C═O of the inhibitor. The Gln192Oϵ hydrogen bonds to Gln192N and to water W57.

The details of interactions in S1 between **2** and trypsin are shown schematically in Figure 4b and graphically in Figure 6. The amidine of the SAPA fragment binds to trypsin, making contacts that are very similar to those seen for the amidine portion of the Arg fragment in **1**. These include the two hydrogen bonds to Asp189COO^- and hydrogen bonds to Gly219 and Ser190Oγ (see Figure 4a,b). The last hydrogen bond is a consequence of the Ser190/Ala190 difference between trypsin and thrombin. Thus, it is present in the trypsin complexes of both **1** and **2**. In thrombin the corresponding hydrogen bond is to a water molecule, identified as W38 in Figure 3a,b.

The segment with important differences in binding of **1** and **2** to trypsin are highlighted with boxes in Figure 4a,b. The internal nitrogen in SAPA is substituted fully with alkyl groups and hence does not make a hydrogen bond to solvent. This change in hydrogen bond to bound water is seen when **1** and **2** bind to thrombin as well and is not unique to trypsin (hydrogen bonds to W65 are present in Figures 3a and 4a and are absent in Figures 3b and 4b).

The second and critical difference is the interaction between the inhibitor and Gln192 of trypsin. In the trypsin complex with **2**, there is no hydrogen bond between the P2 C═O on the inhibitor and Gln192Nϵ due to the potential for VDW clash between the trimethylene bridge in **2** and Gln192Nϵ. To accommodate the trimethylene bridge in **2**, the distance between P2 C═O and Gln192Nϵ increases to 5.61 Å and the χ1 angle[27] of Gln192 changes from −90° to 62°. Presumably, this angle change causes less strain than a significant movement of backbone atoms of residue Gln192. The change in χ1 also causes a movement ranging from 2.8 to 3.3 Å for the Cδ, Oϵ1, and Nϵ2 atoms of Gln192 in the trypsin complex of **2** when compared to that of **1**. This is illustrated in Figure 6 by the minimal overlap of the Connolly surfaces (yellow for **1** and cyan for **2**). In the trypsin complex of **2**, Gln192O no longer hydrogen bonds to Gln192N, but hydrogen bonds to Asn143Nδ. In addition, Gln192Nϵ and Gln192N are surrounded by inhibitor methylene atoms and the Cys191−Cys220 disulfide bridge, respectively, removing the possibility of their hydrogen bonding to solvent.

In summary, the change in Gln192 χ1 angle leaves three amide protons without hydrogen bond partners, which should increase the enthalpy of the complex. Since two of those participate in strong hydrogen bonds in the trypsin complex of **1** (with P2 C═O on the

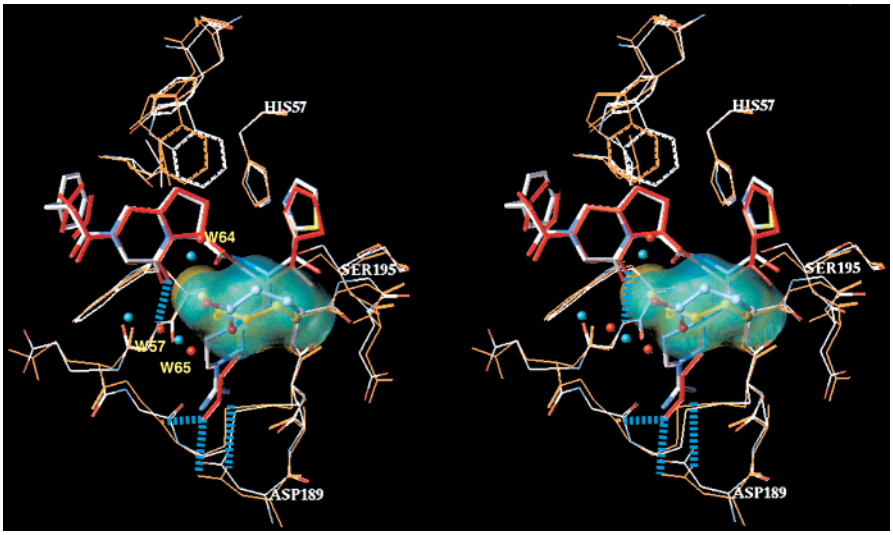

Figure 5. Stereographic representation of the substrate site of thrombin−**1** and thrombin−**2** complexes shown overlapped. Thrombin of thrombin−**1** complex is shown in orange (thin lines), and residue Glu192 is highlighted as orange ball-and-stick. Its Connolly surface is represented in translucent yellow. Inhibitor **1** is shown in red orange (thick lines), and select intermolecular hydrogen bonds are highlighted in cyan. Selected water molecules in the vicinity of the S1 pocket are shown as red spheres. Thrombin of thrombin−2 complex is shown (thin lines) in atom-type based coloring (C = white, O = red, N = blue, S = yellow), and residue Glu192 is highlighted as ball-and-stick and its Connolly surface is shown in translucent cyan. Inhibitor **2** is shown (thick lines) in atom-type based coloring (see above for color code). Selected water molecules in the vicinity of S1 site are shown as cyan spheres.

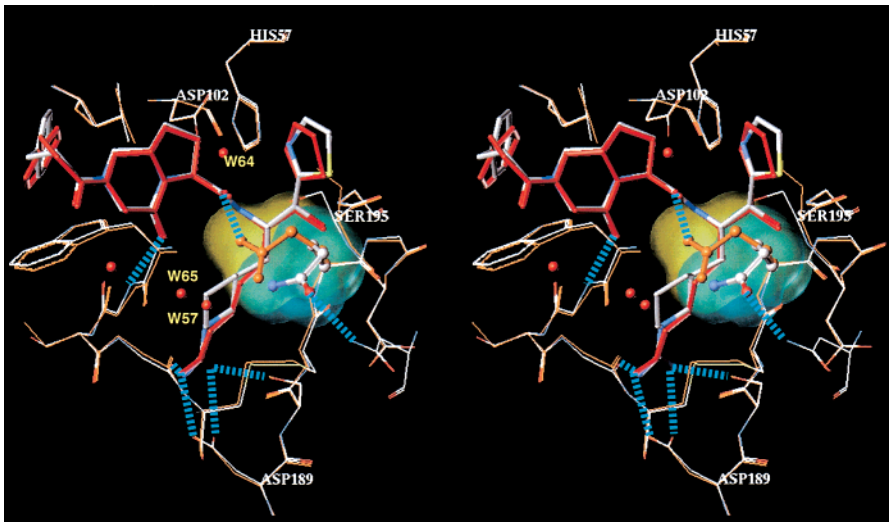

Figure 6. Stereographic representation of the substrate site of trypsin−**1** and trypsin−**2** complexes shown overlapped. Trypsin of trypsin−**1** complex is shown in orange (thin lines), and residue Gln192 is highlighted as orange ball-and-stick. Its Connolly surface is represented in translucent yellow. Inhibitor **1** is shown in red orange (thick lines), and select intermolecular hydrogen bonds are highlighted in cyan. Selected water molecules in the vicinity of the S1 pocket are shown as red spheres. Trypsin of trypsin−**2** complex is shown (thin lines) in atom-type based coloring (C = white, O = red, N = blue, S = yellow), and residue Gln192 is highlighted as ball-and-stick and its Connolly surface is shown in translucent cyan. Inhibitor **2** is shown (thick lines) in atom-type based coloring (see above for color code).

inhibitor, and Gln192O of the enzyme), one could expect a significant drop in trypsin binding free energy for **2** relative to **1**, consistent with a 4350-fold increase in IC_{50} to 4350 nM from <1 nM.

Comparison of Thrombin and Trypsin Binding for 1. A comparison of binding in thrombin and trypsin complexes of **1** (Figures 3a and 4a) reveals two significant differences. First, Ser190Oγ of trypsin accepts a hydrogen bond from the inhibitor, while in thrombin, water W38 is the acceptor. This arises from a sequence difference between trypsin (Ser190) and thrombin (Ala190) and suggests that amidine ligands might be slightly more potent against trypsin than thrombin due to this intermolecular hydrogen bond to Ser190Oγ.

Second, water W65 (See figures 3a and 4a), which hydrogen bonds to the arginine internal nitrogen, donates a hydrogen bond to Glu192COO^- oxygen in the thrombin complex but hydrogen bonds to Gly219O (2.8 Å) in the trypsin complex. Since this water accepts a hydrogen bond from an electropositive arginine nitrogen, charge complementarity favors it to hydrogen bond with the most electronegative atom available. In the thrombin complex, the choice is between Glu192COO^- and Gly219O, and the former is preferred. In the trypsin complex, the choice is between Gly219O and Gln192Nϵ, and Gly219O is preferred. This observed binding difference is a direct consequence of the sequence difference at 192, glutamic acid in thrombin vs glutamine in

Table 1. Comparison of Solvent Accessible Surface Area Occluded on Complex Formation (in Å^2)

buried area	thr−**1**	thr−**2**	try−**1**	try−**2**	thr−**2** vs −**1**	try−**2** vs −**1**
polar	649	627	672	573	−22	−99
apolar	365	481	404	491	+116	+87
total	1013	1108	1075	1065	+95	−12
affinity IC_50	5 nM	30 nM	<1 nM	4350 nM		

trypsin, but has little influence on selectivity since **1** binds to trypsin and thrombin with comparable potency.

Comparison of Thrombin and Trypsin Binding for 2. The hydrogen bonds between **2** and water W38 in the thrombin complex and between **2** and Ser190Oγ in the trypsin complex (see Figures 3b and 4b) are caused by the sequence difference at residue 190 which has been discussed previously, in the context of complexes with **1**. Second, in either complex with **2**, there is no room for water W65, since it is displaced by inhibitor methylene atoms.

One significant difference between the two complexes is the contact between the methylene bridge of the inhibitor and the residue at 192. In the thrombin complex, Glu192COO$^-$ makes VDW contact with the inhibitor methylene atoms via one oxygen and hydrogen bonds to water W57 via the other. In the trypsin complex, Gln192Nϵ does not make VDW contact with the methylene atoms of inhibitor and is so juxtaposed between the inhibitor and the Cys191−Cys220 disulfide bridge that it cannot hydrogen bond to solvent. In comparison to the corresponding complex with **1**, the Glu192COO$^-$ of thrombin loses the interaction with water W65 and gains the interaction with the inhibitor methylene atoms. While there seems to be nothing obvious that prevents the Gln192Nϵ of trypsin from making VDW contact with the inhibitor methylene similar to Glu192COO$^-$, it is possible that the aliphatic hydrogen atoms of the amidinopiperidine are slightly electropositive which would explain the attraction to Glu192COO$^-$ in the thrombin complex and possible repulsion of Gln192Nϵ in the trypsin complex.

Comparison of Buried Apolar and Polar Surfaces on Enzyme and Inhibitor. The magnitude and character of the solvent accessible surface area[28,29] of the enzymes (and ligands) occluded from solvent on complex formation were studied to obtain a more complete evaluation of the enzyme−inhibitor interfaces. The results, as shown in Table 1 and discussed below, were consistent with, and elaborated upon, the conclusions reached from the study of the hydrogen bonding patterns.

The buried polar surface decreases by 22 Å^2 in thrombin−**2** when compared to thrombin−**1**. The corresponding change for trypsin−**2** is a decrease of 99 Å^2 of buried polar surface area from that calculated for trypsin−**1**. The reduction of 22 Å^2 in the case of thrombin is consistent with the earlier observation that there is very little change in enzyme−inhibitor hydrogen bonding between thrombin−**1** and thrombin−**2** complexes (highlighted in Figure 3a,b). In the case of the trypsin complexes, the markedly large decrease of 99 Å^2 emphasizes the earlier observation that there is a significant reduction of enzyme−inhibitor hydrogen bonds in trypsin−**2** compared to trypsin−**1** (Figure 4a,b).

Ligand **2** is less polar, and the nature of the variation in buried apolar surface area among the complexes can contribute to selectivity. A comparison of the change in apolar surface area provides an additional detail on the origin of the thrombin selectivity of **2**. The increase in buried apolar surface (see Table 1) going from thrombin−**1** to thrombin−**2** is 116 Å^2 and is larger than the 87 Å^2 increase calculated for the corresponding trypsin complexes. This suggests that the extra methylenes in **2** may be contributing to selectivity through larger hydrophobic binding to thrombin.

Table 2. Solvent Accessible Surface Area (in Å^2) for the Bound Conformation of **1** and **2** in Their Complexes with Thrombin and Trypsin

accessible surface	**1** in thrombin−**1**	**1** in trypsin−**1**	**2** in thrombin−**2**	**2** in trypsin−**2**
polar	267	260	233	231
apolar	528	531	586	577
total	795	790	819	809
affinity (IC_{50})	5 nM	<1 nM	30 nM	4350 nM

In summary, the surface area calculations corroborate the structural observation that there is one less protein−ligand hydrogen bond in trypsin−**2** compared to trypsin−**1**. In addition, change in buried apolar surfaces suggests a slightly higher hydrophobic binding for thrombin−**2** over trypsin−**2**.

Comparison of Bound Small Molecule Conformations. The thrombin-bound conformations[30] of **1** and **2** are superimposable with a root-mean-square deviation (root-mean-square deviation, abbreviated to RMSD, is a measure of mean distance between two groups of atoms) of 0.47 Å for the corresponding heavy atoms (0.23 Å for the common heavy atoms in the arginine and SAPA fragments), underscoring the strong similarity in binding conformation present in the two complexes. The trypsin-bound conformations of **1** and **2** are superimposable with an RMSD of 0.41 Å for all corresponding heavy atoms (0.18 Å for common heavy atoms of arginine and SAPA fragments). The trypsin and thrombin-bound conformations of **1** differ with an RMSD of only 0.43 Å (0.20 Å for the arginine heavy atoms only), and the corresponding number for **2** is 0.5 Å (0.18 Å for the SAPA heavy atoms only).

The small RMS deviations for the trypsin- and thrombin-bound conformations of **1** and **2** and the smaller deviations for the common heavy atoms of their arginine or SAPA fragments suggests that the binding conformations of the common portions of these two molecules are very similar with both enzymes. The solvent accessible surface areas for **1** in its thrombin- and trypsin-bound conformations are very close as shown in Table 2. The same conclusion follows from the surface areas for **2**, also in Table 2. The very similar surface areas for the thrombin and trypsin binding conformations of the individual compounds supports the conclusion from the RMSD values that the binding conformations are very similar.

The Role of Gln192 and Ser190 of Trypsin. The structural details, discussed previously, show that

Table 3. Summary of Distances Observed between Gln192Nϵ and P2 C=O Oxygen in a Set of 24 Trypsin−Inhibitor Complexes Found in the PDB and Their Comparison to Corresponding Distances in Trypsin Complexes of **1** and **2**

structure/s	Gln192Nϵ to P2 C=O dist. (Å)	comments
17[a] structures from PDB	2.89 ± 0.15	hydrogen bond present
7[b] structures from PDB	5.61 ± 0.9	closer approach of Gln192 Nϵ and P2 C=O blocked by other atoms on the inhibitors
trypsin−**1** complex	2.35	hydrogen bond present
trypsin−**2** complex	5.51	closer approach of of Gln192 Nϵ and P2 C=O blocked by C1 on the trimethylene bridge

[a] These 17 structures have the following PDB codes: 1BRB, 1BRC, 1PPE, 1TPA, 1TPS, 1TYN, 1AN1, 1AQ7, 1BTW, 1BTX, 1BTZ, 1FXY, 1JRS, 1JRT, 1LDT, 1SMF, and 1TAW. [b] These seven structures have the following PDB codes: 1TAB, 1MAX, 1MAY, 1SLU, 1SLV, 1SLW, 1SLX.

Gln192 of trypsin adopts a very different conformation in the trypsin−**2** complex as compared to the trypsin−**1** complex, resulting in loss of intermolecular and intramolecular hydrogen bonds. Glutamic acid 192 of thrombin changes conformation very little between its complexes with **1** and **2**, leading to the conclusion that this sequence difference between the two enzymes plays a large role in the selectivity observed.

An active role for Gln192 of trypsin in ligand/substrate specificity is in agreement with results from other studies that have implicated the corresponding residue in thrombin,[31] protein C,[32] and tissue factor VIIa[33] in determining substrate specificity. While no such direct study exists for trypsin, a survey of structures of trypsin−inhibitor complexes available in the PDB,[34] where the inhibitor contains a P2 carbonyl, was undertaken to study the frequency and nature of intermolecular hydrogen bond formation between Gln192Nϵ and P2 C=O. The results are shown in Table 3.

In 17 of the 24 instances, the interatomic distance between Gln192Nϵ and P2 C=O oxygen is 2.89 ± 0.15 Å, indicating the presence of a strong hydrogen bond. In 7 of the 24 cases, the corresponding distance is 5.61 ± 0.9 Å and the hydrogen bond is absent. In all the latter seven cases, it is clear that the Gln192Nϵ of trypsin is blocked from closer approach to the P2 C=O oxygen due to the potential for VDW overlap with one or more atoms on the inhibitor. This bears similarity to what is seen in the trypsin−**2** complex, where the methylene atoms on the inhibitor interfere with the formation of this intermolecular hydrogen bond. The distance seen in the trypsin−**2** complex, 5.51 Å, is in the range of what is observed in these seven structures. The spatial position of Gln192 atoms in these seven structures is also similar to what is seen in the trypsin−**2** complex.

The data on these 24 structures show that what is observed in the trypsin−**2** complex is part of a trend and is not unique to our structure. Further, the data in Table 3 strongly support the precept that the intermolecular hydrogen bond between P2 C=O on the inhibitor and Gln192Nϵ on trypsin is consistently formed and is absent only when there is interference by other inhibitor atoms. These results support our hypothesis that the disruption of the intermolecular hydrogen bond involving Gln192 of trypsin plays a role in the lowered activity of **2** toward trypsin.

The other sequence difference between thrombin and trypsin in the vicinity of S1, Ala190 in thrombin in comparison to Ser190 in trypsin, does not seem to contribute to selectivity since there is very little change in the spatial location or the nonbonded interactions of Ala190 and Ser190 of the respective enzymes between their complexes with **1** and **2**. In this regard, the inhibition of the catalytic activity of factor Xa by **1** and **2** provides an interesting contrast since factor Xa has a glutamine at 192 and an alanine at 190, differing partially from thrombin and trypsin, respectively. The structure[35] of factor Xa is available, and its S1 pocket is structurally very similar to that of thrombin and trypsin. The activity profile of **1** and **2** against factor Xa could be expected to be similar to trypsin if Gln192 has a stronger role in the differential binding and similar to that of thrombin if Ala190 does. The IC_{50} data for **1** and **2** against factor Xa are 30 nM and 115 000 nM (3800-fold difference), respectively, strongly paralleling the profile seen with trypsin and in agreement with previous reports[20] on factor Xa activity for compounds containing the SAPA fragment. The activity profile against factor Xa is supportive of our conclusion that Gln192 of trypsin has a major role in causing the selectivity of this P1 fragment and that the sequence difference at position 190 has, if any, a minor role.

Conclusion

In summary, we have identified the factors responsible for the selectivity resulting from the replacement of the P1 arginyl fragment of a nonselective inhibitor such as **1** with the SAPA fragment. The structural data show that the introduction of this fragment selectively disturbs the pattern of hydrogen bonding observed for the trypsin−**1** complex, reducing the number of enzyme−inhibitor hydrogen bonds and burying two potentially hydrogen bonding groups into apolar surfaces. In addition, the hydrophobic trimethylene chain of **2** causes a relatively larger increase in buried apolar surface area in the thrombin complex. The sum of these two effects causes the reduction of potency against trypsin while leaving thrombin affinity mostly unchanged.

The structural data also suggest that Gln192 of trypsin plays a major role in the selectivity observed. It is of note that the activity ratio for **1** and **2** against factor Xa is very similar to the activity ratio against trypsin. Since factor Xa also has a glutamine at position 192, the factor Xa activity profile is consistent with the conclusion that the selectivity is related to the sequence at position 192 and suggests that all trypsin-like serine proteases with Gln192 might show reduced affinity for inhibitors containing the SAPA fragment.

Experimental Section

Chemistry. The compounds **1** and **2** were synthesized by methods published previously.[23,24]

Table 4. Crystallographic Data Collection and Refinement Statistics for Complexes

	thrombin		trypsin	
inhibitor	**1**	**2**	**1**	**2**
space group	*C*2	*C*2	*P*212121	*P*212121
cell constants				
a (Å)	70.9	70.6	63.7	63.8
b (Å)	72.4	72.4	63.5	63.8
c (Å)	72.9	72.5	69.1	69.1
β (deg)	100.8	100.3	90.0	90.0
data resolution (Å)	2.5	2.5	1.7	1.7
R_{merge} (%)	13.1	7.7	6.6	6.4
R for last shell (%)	51.3	23.9	27.3	34.0
last shell	2.8−2.5	2.8−2.5	1.76−1.7	1.8−1.7
redundancy	2.8	2.7	4.0	7.1
no. unique reflections	12093	10835	29253	29716
completeness (%)	95.6	85.9	93.1	99.0
last shell (%)	98.1	88.3	89.5	93.3
I/σ (last shell)	1.9	4.2	>5.0	3.9
refinement				
no. reflections	12093	10835	27711	19515
resolution (Å)	2.5	2.5	1.7	1.7
no. solvent molecules	90	92	78	71
R-factor (%)	17.7	20.6	20.3	20.9
R_{free} (10% test set)	31.1	30.8	24.1	21.7
rms deviations				
bond lengths (Å)	0.02	0.02	0.018	0.018
bond angles (deg)	3.95	3.93	3.7	3.6

X-ray Crystallography. α-Thrombin from human serum was obtained from Haematologic Technologies Inc. Hirugen fragment 55−65 and bovine trypsin were obtained from Sigma. Crystals of a trypsin−benzamidine complex were grown at room temperature from hanging drops comprised of 4 μL of 40 mg/mL trypsin, 4 μL of well solution, and 0.4 μL of 1 M benzamidine, where the well solution contained 2.5 M $(NH_4)_2SO_4$, 0.01 M $CaCl_2$, and 0.1 M Tris-HCl buffer at pH 7.0. Drops were equilibrated against 600 μL of well solution and produced brick-shaped crystals in 3 days, typically 0.3 mm × 0.3 mm × 1.0 mm in size. Crystals of the thrombin−hirugen complex were obtained by the sitting drop vapor diffusion method. Protein solution (8 μL drops) containing 3.5 mg/mL thrombin−hirugen complex, 50 mM sodium phosphate, pH 7.3, and 10% PEG 8000 were allowed to equilibrate against a reservoir containing 600 μL of 0.1 M sodium phosphate and 20% w/v PEG 8000. Following equilibration for 24 h at room temperature, the protein drops were seeded with small thrombin−hirugen crystals which continued to grow for several months, reaching dimensions of 0.5 mm × 0.5 mm × 0.3 mm.

Inhibitor−trypsin complexes were prepared by soaking preformed trypsin−benzamidine crystal in 300 μL of mother liquor [3.0 M $(NH_4)_2SO_4$, 0.01 M $CaCl_2$, and 0.1 M Tris-HCl buffer, pH 7.0] for 1 day and exchanging this mother liquor twice with some containing a saturating amount of inhibitor (1 mg/mL); the second exchange was after 1 day. The total soak time was 3 days. Crystals of each complex of thrombin with inhibitor were obtained by soaking pregrown thrombin−hirugen crystals in solution containing 10 mM inhibitor, 0.1 M sodium phosphate, pH 7.3, and 20% PEG 8000 for 24−48 h at 24 ° C.

X-ray diffraction data were collected at room temperature using a MarResearch Image Plate detector and a Rigaku Ru-200B rotating anode X-ray generator operating at 40 kV and 120 mA. Both trypsin complexes are isomorphous with β-trypsin in space group $P2_12_12_1$.[36] The thrombin complexes are isomorphous to the monoclinic hirugen−thrombin crystals in space group C2.[37] Diffraction data were processed using the MarResearch version of XDS. Important data collection statistics and parameters are given in Table 4.

Structures of complexes were determined using difference electron density methods which revealed the positions and conformations of a single bound ligand located in the active site of the respective protein. The β-trypsin structure (PDB entry code 1TLD)[36] including protein, waters, and Ca^{2+} ions, but without the sulfate molecule, was used as a starting model for trypsin complexes. The published coordinates for the unliganded thrombin−hirugen structure (PDB entry code 1HGT)[37] were used for the thrombin complexes. Initially, XPLOR was used to refine protein atom positions and individual temperature factors.[38] The position and conformation of the inhibitor in each complex was identified in QUANTA using the residual map phased on the protein refinement. Additionally, individual waters were examined for reasonable temperature factors and positions, while new waters were added based on appropriate peaks in the fo-fc map making reasonable hydrogen bonds. A final round of refinement was carried out for each complex including the protein, inhibitor, and solvent. Relevant refinement statistics are shown in Table 4.

Molecular Modeling. Molecular graphics operations and geometry measurements were accomplished using the Sybyl molecular modeling package (Version 6.4) from Tripos Inc., St. Louis, MO. The solvent accessible surface area (SASA) data were calculated using Connolly's MSAREA[29] program from the three-dimensional coordinates of the complexes. A probe of size 1.4 Å was used. The SASA values were calculated for the apo protein, the ligand (in its binding conformation), and the complex separately. The SASA values for the complex was subtracted from the sum of the individual SASA for the apo protein and ligand to obtain the SASA occluded on binding. The coordinates of thrombin, present in PDB entry 1HAH, was used as apo protein for thrombin complexes, and the coordinates of trypsin, present in PDB entry 2PTN, were used for trypsin complexes. The structures in PDB entries 1HAH and 2PTN do not have any ligand bound in their substrate site, and their structure closely resembles that of the thrombin and trypsin structures present in the complexes. The apolar and polar characterization was based on atom types. Surface points in contact with carbon or sulfur were considered apolar, and surfaces in contact with oxygen or nitrogen were considered polar.

Chromogenic Assay. Thrombin Inhibition. The inhibition of catalytic activity of thrombin by a compound was assessed by determination of its concentration that inhibits the thrombin cleavage of the chromogenic substrate Chromozym TH (Tos-Gly-Pro-Arg-*p*-nitroanilide acetate from Boehringer Mannheim) at the 50% level. Typically, 145 μL of human thrombin (0.75 nM, from Enzyme Research Laboratories) in HPB buffer (10 mM HEPES, with 100 mM NaCl, 0.05% bovine serum albumin, and 0.1% PEG-8000, pH 7.4) and 5 μL of the test compound in DMSO (2% final) were incubated for 60 min at room temperature. To this mixture was added 100 μL of Chromozym TH (24 μM final) in HPB buffer, and the velocity of Chromozyme TH hydrolysis was obtained by measuring absorbance at 405 nM every 10 s for 5 min using a ThermoMax Kinetic Microplate Reader.

Trypsin Inhibition. The inhibition of catalytic activity of trypsin by a compound was assessed by determination of its concentration that inhibits the trypsin cleavage of the chromogenic substrate S2222 (Bz-Ile-Glu-Gly-Pro-Arg-*p*-nitroanilide HCl, from Diapharma) at the 50% level. Typically, 145 μL of human trypsin (0.5 nM final, in 10 mM HEPES, with 100 mM NaCl, 0.05% bovine serum albumin, and 0.1% PEG-8000) and 5 μL of test substance in DMSO (2% final) were incubated for 60 min at room temperature. To this mixture was added 100 μL of S2222 in HBSA buffer (100 μM final), and the velocity of S2222 hydrolysis was obtained by measuring absorbance at 405 nM every 10 s for 5 min using a ThermoMax Kinetic Microplate Reader.

Factor Xa Inhibition. The inhibition of catalytic activity of factor Xa by a compound was assessed by determination of its concentration that inhibits the factor Xa cleavage of the chromogenic substrate S2765 (N-CBz-DArg-LGly-LArg-*p*-nitroanilide 2HCl, from Diapharma) at the 50% level. Typically, 145 μL of human factor Xa (1 nM final, from Enzyme Research Laboratories), in HBSA buffer (10 mM HEPES, with 150 mM NaCl, 0.05% bovine serum albumin, and 0.1% PEG-8000), and 5 μL of test substance in DMSO (2% final) were incubated for

60 min at room temperature. After this mixture was preheated to 37 °C for 5 min, 100 μL of S2765 in HBSA buffer (400 μM final) was added, and the velocity of S2765 hydrolysis was obtained by measuring absorbance at 405 nM every 10 s for 5 min using a ThermoMax Kinetic Microplate Reader.

Acknowledgment. We thank Mark Snow, Ph.D., for useful discussions and critical readings of the manuscript.

References

(1) Davie, E. W.; Fujikawa, K.; Kisiel, W. The coagulation cascade: initiation, maintenance, and regulation. *Biochemistry* **1991**, *30*, 10363−70.
(2) Fenton, J. W., II; Ofosu, F. A.; Moon, D. G.; Maraganore, J. M. Thrombin structure and function: why thrombin is the primary target for antithrombotics. *Blood Coagulation Fibrinolysis* **1991**, *2*, 69−75.
(3) Maraganore, J. M. Thrombin, thrombin inhibitors, and the arterial thrombotic process. *Thromb. Haemostasis* **1993**, *70*, 208−11.
(4) Maraganore, J. M. Hirudin and hirulog: Advances in antithrombotic therapy. *Perspect. Drug Discovery Des.* **1994**, *1*, 461−78.
(5) Ripka, W. C.; Vlasuk, G. P. Antithrombotics/serine proteases. *Annu. Rep. Med. Chem.* **1997**, *32*, 71−89.
(6) Kaiser, B. *Drugs Future* **1998**, *23*, 423−436.
(7) Menear, K. *Curr. Med. Chem.* **1998**, *5*, 457−468.
(8) Vacca, J. P. *Annu. Rep. Med. Chem.* **1998**, *33*, 81−90.
(9) Kimball, S. D. *Handb. Exp. Pharmacol.* **1999**, *132*, 367−396.
(10) De Nanteuil, G.; Verbeuren, T. J. *Expert Opin. Invest. Drugs* **1999**, *8*, 173−180.
(11) Hauptmann, J.; Sturzebecher, J. *Thromb. Res.* **1999**, *93*, 203−241.
(12) Sanderson, P. E. J. *Med. Res. Rev.* **1999**, *19*, 179−197.
(13) Menear, K. *Expert Opin. Invest. Drugs* **1999**, *8*, 1373−1384.
(14) Rydel, T. J.; Ravichandran, K. G.; Tulinsky, A.; Bode, W.; Huber, R.; Roitsch, C.; Fenton, J. W., II. The structure of a complex of recombinant hirudin and human.alpha.-thrombin. *Science (Washington, D. C., 1883-)* **1990**, *249*, 277−80.
(15) Bode, W.; Turk, D.; Karshikov, A. The refined 1.9-.ANG. X-ray crystal structure of D-Phe-Pro-Arg chloromethylketone-inhibited human.alpha.-thrombin: structure analysis, overall structure, electrostatic properties, detailed active-site geometry, and structure−function relationships. *Protein Sci.* **1992**, *1*, 426−71.
(16) Bode, W.; Turk, D.; Stuerzebecher, J. Geometry of binding of the benzamidine- and arginine-based inhibitors N.alpha.-(2-naphthyl-sulfonyl-glycyl)-DL-p-amidinophenylalanyl-piperidine (NAPAP) and (2R, 4R)-4-methyl-1-[N.alpha.-(3-methyl-1,2,3,4-tetrahydro-8-quinolinesulfonyl)-L-arginyl]-2-piperidine carboxylic acid (MQPA) to human.alpha.-thrombin. X-ray crystallographic determination of the NAPAP-trypsin complex and modeling of NAPAP-thrombin and MQPA-thrombin. *Eur. J. Biochem.* **1990**, *193*, 175−82.
(17) Turk, D.; Stuerzebecher, J.; Bode, W. Geometry of binding of the N.alpha.-tosylated piperidides of m-amidino-, p-amidino- and p-guanidino phenylalanine to thrombin and trypsin. X-ray crystal structures of their trypsin complexes and modeling of their thrombin complexes. *FEBS Lett.* **1991**, *287*, 133−8.
(18) St. Laurent, D. R.; Balasubramanian, N.; Han, W. T.; Trehan, A.; Federici, M. E.; Meanwell, N. A.; Wright, J. J.; Seiler, S. M. Active site-directed thrombin inhibitors. II. Studies related to arginine/guanidine bioisosteres. *Bioorg. Med. Chem.* **1995**, *3*, 1145−56.
(19) Hilpert, K.; Ackermann, J.; Banner, D. W.; Gast, A.; Gubernator, K.; Hadvary, P.; Labler, L.; Mueller, K.; Schmid, G.; Tschopp, T. B.; Waterbeemd, H. v. d. Design and Synthesis of Potent and Highly Selective Thrombin Inhibitors. *J. Med. Chem.* **1994**, *37*, 3889−901.
(20) Levy, O. E.; Semple, J. E.; Lim, M. L.; Reiner, J.; Rote, W. E.; Dempsey, E.; Richard, B. M.; Zhang, E.; Tulinsky, A.; Ripka, W. C.; Nutt, R. F. Potent and Selective Thrombin Inhibitors Incorporating the Constrained Arginine Mimic L-3-Piperidyl-(N-guanidino)alanine at P1. *J. Med. Chem.* **1996**, *39*, 4527−4530.
(21) Semple, J. E.; Rowley, D. C.; Brunck, T. K.; Ha-Uong, T.; Minami, N. K.; Owens, T. D.; Tamura, S. Y.; Goldman, E. A.; Siev, D. V.; Ardecky, R. J.; Carpenter, Y. G.; Richard, B. M.; Nolan, T. G.; Hakanson Kjell; Tulinsky, A.; Nutt, R. F.; Ripka, W. C. Design, Synthesis, and Evolution of a Novel, Selective, and Orally Bioavailable Class of Thrombin Inhibitors: P1−Argininal Derivatives Incorporating P3−P4 Lactam Sulfonamide Moieties. *J. Med. Chem.* **1996**, *39*, 4531−4536.
(22) Krishnan, R.; Zhang, E.; Hakansson, K.; Arni, R. K.; Tulinsky, A.; Lim-Wilby, M. S. L.; Levy, O. E.; Semple, J. E.; Brunck, T. K. Highly Selective Mechanism-Based Thrombin Inhibitors: Structures of Thrombin and Trypsin Inhibited with Rigid Peptidyl Aldehydes. *Biochemistry* **1998**, *37*, 12094−12103.
(23) St-Denis, Y.; Augelli-Szafran, C. E.; Bachand, B.; Berryman, K. A.; DiMaio, J.; Doherty, A. M.; Edmunds, J. E.; Leblond, L.; Levesque, S.; Narasimhan, L. S.; Penvose-Yi, J. R.; Rubin, J. R.; Tarazi, M.; Winocour, P. D.; Siddiqui, M. A. Potent Bicyclic Lactam Inhibitors of Thrombin: Part I: P3 Modifications. *Bioorg. Med. Chem.* **1998**, *8*, 3193−3198.
(24) Plummer, J. S.; Berryman, K. A.; Cai, C.; Cody, W., L.; DiMaio, J.; Doherty, A., M.; Eaton, S.; Edmunds, J. J.; He, J. X.; Holland, D. R.; Lafleur, D.; Levesque, S.; Narasimhan, L. S.; Rubin, J. R.; Rapundalo, S. T.; Siddiqui, M. A.; Susser, A.; St-Denis, Y.; Winocour, P. Potent and Selective Bicyclic Lactam Inhibitors of Thrombin: Part 2: P1 Modifications. *Bioorg. Med. Chem.* **1998**, *8*, 3409−3414.
(25) Schechter, I.; Berger, A. On the size of the active site in proteases. I. Papain. *Biochem. Biophys. Res. Commun.* **1967**, *27*, 157−62.
(26) Nakayama, Y.; Senokuchi, K.; Nakai, H.; Obata, T.; Kawamura, M. Therapeutic potential of trypsin-like serine protease inhibitors. *Drugs Future* **1997**, *22*, 285−293.
(27) Schulz, G. E.; Schirmer, R. H. *Principles of Protein Structure*; Springer-Verlag: New York, 1979.
(28) Richards, F. M. Calculation of molecular volumes and areas for structures of known geometry. *Methods Enzymol.* **1985**, *115*, 440−64.
(29) Connolly, M. L. The molecular surface package. *J. Mol. Graphics* **1993**, *11*, 139−41.
(30) Note: Crystallographically obtained conformations of small molecules present as receptor complexes tend to have small variations in bond lengths, bond angles, and torsions from canonical values used by molecular mechanics force fields. This could translate to large strain energies when evaluated using molecular mechanics. Proper treatment of strain energies across four enzyme complexes where the inhibitors are covalently attached to the enzyme is beyond the scope of this work. Hence a comparison of strain energies for the bound conformations of the inhibitors is not considered.
(31) Le Bonniec, B. F.; Esmon, C. T. Glu-192→Gln substitution in thrombin mimics the catalytic switch induced by thrombomodulin. *Proc. Natl. Acad. Sci. U.S.A.* **1991**, *88*, 7371−5.
(32) Guinto, E. R.; Ye, J.; Le Bonniec, B. F.; Esmon, C. T. Glu192→Gln substitution in thrombin yields an enzyme that is effectively inhibited by bovine pancreatic trypsin inhibitor and tissue factor pathway inhibitor. *J. Biol. Chem.* **1994**, *269*, 18395−400.
(33) Neuenschwander, P. F.; Morrissey, J. H. Alteration of the Substrate and Inhibitor Specificities of Blood Coagulation Factor VIIa: Importance of Amino Acid Residue K192. *Biochemistry* **1995**, *34*, 8701−7.
(34) Abola, E. E.; Sussman, J. L.; Prilusky, J.; Manning, N. O. Protein Data Bank archives of three-dimensional macromolecular structures. *Methods Enzymol.* **1997**, *277*, 556−571.
(35) Padmanabhan, K.; Padmanabhan, K. P.; Tulinsky, A.; Park, C. H.; Bode, W.; Huber, R.; Blankenship, D. T.; Cardin, A. D.; Kisiel, W. Structure of human Des(1−45) factor Xa at 2.2.ANG. resolution. *J. Mol. Biol.* **1993**, *232*, 947−66.
(36) Bartunik, H. D.; Summers, L. J.; Bartsch, H. H. Crystal structure of bovine.beta.-trypsin at 1.5.ANG. resolution in a crystal form with low molecular packing density. Active site geometry, ion pairs and solvent structure. *J. Mol. Biol.* **1989**, *210*, 813−28.
(37) Skrzypczak-Jankun, E.; Carperos, V. E.; Ravichandran, K. G.; Tulinsky, A.; Westbrook, M.; Maraganore, J. M. Structure of the hirugen and hirulog 1 complexes of.alpha.-thrombin. *J. Mol. Biol.* **1991**, *221*, 1379−93.
(38) Brunger, A. T. *X-PLOR Version 3.1 manual*; Yale University Press: New Haven, CT, 1992.

JM990216F